



## UWS Academic Portal

### **DNA sequence-selective C8-linked pyrrolobenzodiazepine(PBD)-heterocyclic polyamide conjugates show anti-tubercular specific activities**

Brucoli, Federico; D. Guzman, Juan; Basher, Mohammad A. ; Evangelopoulos, Dimitrios; McMahon, Eleanor; Munshi, Tulika; McHugh, Timothy D.; Fox, Keith R. ; Bhakta, Sanjib

*Published in:*  
The Journal of Antibiotics

*DOI:*  
[10.1038/ja.2016.43](https://doi.org/10.1038/ja.2016.43)

Published: 31/12/2016

*Document Version*  
Peer reviewed version

[Link to publication on the UWS Academic Portal](#)

#### *Citation for published version (APA):*

Brucoli, F., D. Guzman, J., Basher, M. A., Evangelopoulos, D., McMahon, E., Munshi, T., McHugh, T. D., Fox, K. R., & Bhakta, S. (2016). DNA sequence-selective C8-linked pyrrolobenzodiazepine(PBD)-heterocyclic polyamide conjugates show anti-tubercular specific activities. *The Journal of Antibiotics*, 69, 843-849.  
<https://doi.org/10.1038/ja.2016.43>

#### **General rights**

Copyright and moral rights for the publications made accessible in the UWS Academic Portal are retained by the authors and/or other copyright owners and it is a condition of accessing publications that users recognise and abide by the legal requirements associated with these rights.

#### **Take down policy**

If you believe that this document breaches copyright please contact [pure@uws.ac.uk](mailto:pure@uws.ac.uk) providing details, and we will remove access to the work immediately and investigate your claim.

**DNA sequence-selective C8-linked pyrrolobenzodiazepine(PBD)-heterocyclic polyamide  
conjugates show anti-tubercular specific activities**

Federico Brucoli,<sup>1\*</sup> Juan D. Guzman,<sup>2,†‡</sup> Mohammad A. Basher,<sup>4‡</sup> Dimitrios Evangelopoulos,<sup>2,3‡</sup>  
Eleanor McMahon,<sup>2</sup> Tulika Munshi,<sup>2‡</sup> Timothy D. McHugh,<sup>3</sup> Keith R. Fox,<sup>4</sup> and Sanjib Bhakta<sup>2</sup>

**Author Affiliations**

<sup>1</sup>*School of Science, Institute of Biomedical and Environmental Health Research (IBEHR), University  
of the West of Scotland, Paisley, PA1 2BE, Scotland, UK;* <sup>2</sup>*Department of Biological Sciences,  
Institute of Structural and Molecular Biology, Birkbeck College, University of London, London,  
WC1E 7HX, UK;* <sup>3</sup>*Centre for Clinical Microbiology, University College London, London, NW3 2PF,  
UK;* <sup>4</sup>*Centre for Biological Sciences, University of Southampton, Southampton SO17 1BJ, UK.*

\*Corresponding author. Tel: +44-(0)141-848-3264; E-mail: [federico.brucoli@uws.ac.uk](mailto:federico.brucoli@uws.ac.uk)

**Present addresses:**

<sup>†</sup>Departamento de Química y Biología, Universidad del Norte, Km 5 vía Puerto Colombia,  
Barranquilla 081007, Colombia.

<sup>‡</sup>The Francis Crick Institute, Mill Hill Laboratory, The Ridgeway, Mill Hill, London, NW7 1AA, UK.

<sup>‡</sup>Institute of Infection and Immunity, St George's, University of London, Cranmer Terrace, London  
SW17 0RE, UK.

<sup>‡</sup>These two authors equally contributed to this study.

## Abstract

New chemotherapeutic agents with novel mechanisms of action are in urgent need to combat the tuberculosis pandemic. A library of twelve C8-linked pyrrolo[2,1-c][1,4]benzodiazepine(PBD)-heterocyclic polyamide conjugates (**1-12**) was evaluated for anti-tubercular activity and DNA sequence selectivity. The PBD-conjugates were screened against slow-growing *Mycobacterium bovis* BCG and *M. tuberculosis* H<sub>37</sub>Rv and fast-growing *Escherichia coli*, *Pseudomonas putida* and *Rhodococcus* sp. RHA1 bacteria. DNase I footprinting and DNA thermal denaturation experiments were used to determine the molecules' DNA recognition properties. The PBD-conjugates were highly selective for the mycobacterial strains and exhibited significant growth inhibitory activity against the pathogenic *M. tuberculosis* H<sub>37</sub>Rv, with compound **4** showing MIC values (MIC = 0.08 mg/L) similar to those of rifampin and isoniazid. DNase I footprinting results showed that the PBD-conjugates with three heterocyclic moieties had enhanced sequence selectivity and produced larger footprints with distinct cleavage patterns compared to the two-heterocyclic chain PBD-conjugates. DNA melting experiments indicated a covalent binding of the PBD-conjugates to two AT-rich DNA-duplexes containing either a central GGATCC or GTATAC sequence and showed that the polyamide chains affect the interactions of the molecules with DNA. The PBD-C8-conjugates tested in this study have a remarkable anti-mycobacterial activity and can be further developed as DNA-targeted anti-tubercular drugs.

## Keywords

Drug discovery; DNA-minor groove binding agents; Pyrrolobenzodiazepines; Anti-tubercular agents; DNase I footprinting; *Mycobacterium tuberculosis*; HT-SPOTi

## 1. Introduction

Tuberculosis (TB) is a global health challenge, with 9 million new cases and 1.5 million deaths reported in 2013.<sup>1</sup> Furthermore, it is estimated that one third of the world's population is infected with *Mycobacterium tuberculosis*, accounting for a large reservoir of the bacilli.<sup>1</sup> The increasing incidence of TB is also linked to the steady increase in multi-drug and extensively-drug resistant

tuberculosis (MDR/XDR-TB) strains, which renders TB difficult to treat.<sup>1,2</sup> Therefore, new antibiotics with novel and pleiotropic modes of action are urgently needed to combat the TB pandemic, the rise of resistant bacilli and also provide new, safer and shorter drugs regimens. To this end, the complete reconstruction of the *M. tuberculosis* regulatory network<sup>3</sup> has laid the foundation for the development of DNA-targeted anti-mycobacterial agents. The ability of DNA sequence-selective agents to target specific promoter regions of the *M. tuberculosis* DNA can be exploited to disrupt the binding of mycobacterial transcription factors, induce bacterial cell death, overcome antimicrobial resistance and maximize therapeutic efficacy.

DNA-targeted chemotherapeutic agents are an important class of compounds, which have long attracted interest due to their distinctive mode of action involving specific interactions with predetermined DNA sequences.<sup>4-7</sup> Among these agents, pyrrolo[2,1-*c*][1,4]benzodiazepines (PBDs) have played a major role in cancer and antibacterial chemotherapy.<sup>8, 9</sup> PBDs are a family of antitumour-antibiotics first isolated from cultures of *Streptomyces* species.<sup>10</sup> These molecules are DNA sequence-selective agents that covalently bind, via their N10-C11 imine functionality, to the C2-amino groups of guanine residues within the minor groove of DNA, spanning three DNA base pairs with a preference for Pu-G-Pu (where Pu = purine; G = guanine) sequences (**Figure 1**).<sup>9, 11</sup> PBD monomers block transcription by inhibiting RNA polymerase activity in a sequence-specific manner.<sup>12</sup>

Since their discovery, several PBD analogues have been synthesised and extensively evaluated for their anticancer and antibacterial activities.<sup>8, 13-17</sup> However, to our knowledge, there are only few studies focusing on the anti-mycobacterial activity of the PBDs. Taylor and Thurston reported that PBD dimers, in which two PBD units are tethered through a C8/C8'' diether linker to improve DNA-binding affinity and sequence specificity, exhibited notable activity against a panel of rapid and relatively rapid-growing mycobacteria, *Mycobacterium smegmatis*, *M. fortuitum*, *M. abscessus*, *M. phlei* and *M. aurum*.<sup>18</sup> Although showing anti-mycobacterial activity, the PBD dimers displayed significant cytotoxicity against human cell lines, especially compared to PBD monomers, and may be

only used as “drug of last resort” to treat intractable infections caused by multi-drug resistant pathogens.<sup>19</sup> In another study, Kamal *et al.* showed that PBD-5,11-diones (PBD dilactams) inhibited the growth of *Mycobacterium avium*, *M. intracellulare* and *M. tuberculosis*. PBD-dilactams stabilise duplex-DNA to a lesser extent than PBDs, as they lack the N10-C11 imine moiety responsible for the electrophilic alkylation of the C2-NH<sub>2</sub> of guanine bases, thus resulting in a non-covalent DNA interaction and reduced antibacterial and anticancer potency.<sup>9,20</sup>

In the present study, we investigated the anti-mycobacterial activity and DNA binding properties of a library of twelve C8-linked PBD-heterocyclic polyamide conjugates (**1-12**) (**Figure 2**), which were previously shown to have strong *in vitro* anticancer activities.<sup>21-23</sup> The di- or tri-heterocyclic polyamide chains of **1-12** are comprised of combinations of pyrrole (Py), imidazole (Im) and thiazole (Th) rings known for their ability to modulate the ligands’ DNA-binding affinity.<sup>24</sup> C8-linked PBD-polyamide conjugates, unlike PBD dilactams, retain the ability to form covalent DNA-adducts, characteristic responsible for their improved cancer cell cytotoxicity and antibacterial activities,<sup>15</sup> and have a more favourable cytotoxicity profile compared to the PBD dimers.<sup>15,17</sup>

PBD-conjugates **1-12** were screened against slow-growing *Mycobacterium bovis* BCG and *M. tuberculosis* H<sub>37</sub>Rv and fast-growing *Escherichia coli*, *Pseudomonas putida* and *Rhodococcus sp.* and minimum inhibitory concentration values (MIC) were determined. Cytotoxicity against mouse macrophages RAW264.7 was also evaluated. The DNaseI footprinting experiments and thermal denaturation assays were used to evaluate the DNA recognition properties of **1-12**.

## 2. Materials and methods

### *C8-linked PBD-heterocyclic polyamide conjugates*

The twelve PBD-conjugates **1-12** were synthesised and purified using published synthetic routes<sup>21,22</sup> and dissolved in DMSO prior to use.

### *Microorganisms and mammalian cells*

*Mycobacterium bovis* BCG Pasteur (ATCC 35734) and *M. tuberculosis* H<sub>37</sub>Rv (ATCC 27294), and *Escherichia coli* K12 (ATCC 53323), *Pseudomonas putida* KT2442 (ATCC 47054) and *Rhodococcus* sp. RHA1 were used to screen the antibacterial activity of the PBD conjugates. Murine macrophages RAW264.7 (ATCC TIB71) were used in this study to evaluate the cytotoxicity of the PBD-conjugates.

#### *Mammalian macrophage cytotoxicity assay using resazurin assay*

The quantitation of eukaryotic cell toxicity was carried out as previously described.<sup>25</sup>

#### *Antibacterial assay against E. coli, P. putida and Rhodococcus sp.*

The evaluation of growth inhibition of the PDB-conjugates against *E. coli*, *P. putida* and *Rhodococcus* sp. was performed using the spot culture growth inhibition assay (SPOTi) in 24 well plates.<sup>26</sup> A seed culture of each bacteria was prepared in Luria Bertani (LB) broth and grown overnight at 37 °C with shaking at 200 rpm. *Rhodococcus* sp. was grown in LB broth at 30 °C with shaking at 200 rpm. Dilutions of the PBD-conjugates were performed in sterile DMSO at concentrations one thousand-fold more concentrated than the concentrations to be tested. 2 µL of each dilution were dispensed in each well of the 24 well plates, and 2 mL of LB agar were added to each well, and mixed. 2 µL of each inoculum containing approximately 10<sup>5</sup> colony-forming units (CFUs)/mL were carefully dispensed into the middle of the well on the surface of the solidified agar. The plate was incubated overnight at 37 °C for *E. coli* and *P. putida*, and at 30 °C for *Rhodococcus* sp. The plates were visually inspected and minimum inhibitory concentrations (MIC) values were recorded as the lowest concentration of PBD-conjugates where no growth was observed. Kanamycin was included as positive control.

#### *Anti-mycobacterial screening using HT-SPOTi*

*M. bovis* BCG and *M. tuberculosis* H<sub>37</sub>Rv were grown in Middlebrook 7H9 broth supplemented with 0.02% (v/v) glycerol, 0.05% (v/v) tween-80 and 10% (v/v) albumin, dextrose and catalase (ADC; BD

Biosciences) as a rolling culture at 2 rpm and 37 °C, and as a stand culture at 37 °C. The antimycobacterial activities of the compounds were tested following the HT-SPOTi guidelines.<sup>26,27</sup> HT-SPOTi is a high-throughput growth inhibition assay conducted in a semi-automated 96 well plate format. Compounds dissolved in DMSO at a final concentration of 50 mg/mL were serially diluted and dispensed in a volume of 2 µL into each well of a 96 well plate to which 200 µL of Middlebrook 7H10 agar medium kept at 55 °C supplemented with 0.05% (v/v) glycerol and 10% (v/v) OADC was added. Wells with no compounds (DMSO only) and isoniazid (positive control) were used as experimental controls. To all the plates, a drop (2 µL) of mycobacterial culture containing  $2 \times 10^3$  CFUs was spotted in the middle of each well and the plates were incubated at 37 °C for 7 days. The MICs were determined as the lowest concentration of each compound where no mycobacterial growth was observed.

#### *DNase I footprinting assay*

Footprinting reactions were performed as previously described<sup>28</sup> using the DNA fragments HexAfor and HexBRev, which together contain all 64 symmetrical hexanucleotide sequences. The DNA fragments were obtained by cutting the parent plasmids with *Hind*III and *Sac*I (*HexA*) or *Eco*RI and *Pst*I (*HexBRev*) and were labelled at the 3'-end with [ $\alpha$ -<sup>32</sup>P]dATP using reverse transcriptase. After gel purification the radiolabelled DNA was dissolved in 10 mM Tris-HCl pH 7.5 containing 0.1 mM EDTA, at a concentration of about 10 c.p.s per µL as determined on a hand held Geiger counter. 1.5 µL of radiolabelled DNA was mixed with 1.5 µL ligand that had been freshly diluted in 10 mM Tris-HCl pH 7.5, containing 10 mM NaCl. The complexes were left to equilibrate for at least 12 hours before digesting with 2 µL DNase I (final concentration about 0.01 units/ml). The reactions were stopped after 1 minute by adding 4 µL of formamide containing 10 mM EDTA and bromophenol blue (0.1% w/v). The samples were then heated at 100 °C for 3 minutes before loading onto 8% denaturing polyacrylamide gels containing 8 M urea. Gels were fixed in 10% acetic acid, transferred to 3MM paper, dried and exposed to a phosphor screen overnight, before analysing with a typhoon phosphorimager.

149 Fluorescence melting curves were determined in a Roche LightCycler, using a total reaction volume  
150 of 20  $\mu$ L. For each reaction the final oligonucleotide concentration was 0.25  $\mu$ M, diluted in 10 mM  
151 sodium phosphate pH 7.4 containing 100 mM NaCl. The experiments used the duplexes 5'-F-  
152 AAAAGGATCCAAA/5'-TTTTGGATCCTTTT-Q and 5'-F-AAAAGTATACAAA/5'-  
153 TTTTGTATACTTTT-Q (F = fluorescein and Q = dabcy). In a typical experiment the samples were  
154 first denatured by heating to 95 °C at a rate of 0.1 °C s<sup>-1</sup>. The samples were then maintained at 95 °C  
155 for 5 min before annealing by cooling to 25 °C at 0.1 °C s<sup>-1</sup> (this is the slowest heating and cooling  
156 rate for the LightCycler). They were held at 25 °C for a further 5 min and then melted by heating to  
157 95 °C at 0.1 °C s<sup>-1</sup>. Recordings of the fluorescence emission at 520 nm were taken during both the  
158 melting steps as well as during annealing. The data were normalized to show the fractional change in  
159 fluorescence for each sample between the starting and final values. *T<sub>m</sub>* values were determined from  
160 the first derivatives of the melting profiles using the Roche LightCycler software.

### 161 **3. Results**

#### 162 *Growth inhibition of Mycobacterium spp.*

163 In **Table 1** are illustrated the results of the anti-tubercular and anti-bacterial screening, the  
164 cytotoxicity evaluation and the selectivity index (SI) of **1-12**. Compounds **1-12** were tested for  
165 growth inhibition against two slow-growing mycobacteria, *Mycobacterium bovis* BCG and *M.*  
166 *tuberculosis* H<sub>37</sub>Rv. The PBD-conjugates' MIC values against *M. tuberculosis* ranged from 0.08 to  
167 5.19 mg/L, whereas the MIC values against *M. bovis* ranged from 0.04 to 20 mg/L. Dipyrrole-  
168 including PBD-conjugate **4** (Py-Py-PBD) exhibited the highest growth inhibitory activity against *M.*  
169 *tuberculosis* with a MIC value of 0.08 mg/L. Compounds **5** (Py-Py-Im-PBD), **7** (Im-Im-Py-PBD), **9**  
170 (Py-Py-Th-PBD), **10** (Py-Th-Py-PBD) and **12** (Py-Py-Py-PBD) inhibited the growth of *M.*  
171 *tuberculosis* at 0.16 mg/L concentration. PBD-conjugate **1** (Py-Th-PBD) was active against *M.*  
172 *tuberculosis* and *M. bovis* at 0.31 and 0.16 mg/L, respectively, whereas compound **2** (Th-Py-PBD)



inhibited the growth of both mycobacteria at 0.63 mg/L. Compounds **6** (Py-Im-Py-PBD) and **8** (Im-Im-Im-PBD) were found to be 60-fold more active against *M. tuberculosis* (0.32 mg/L) than *M. bovis* BCG (20 mg/L), whereas PBD-conjugates **7**, **9** and **10** were two-fold more active against *M. bovis* (0.08 mg/L) than *M. tuberculosis* (0.16 mg/L). Pyrrole-including PBD-conjugates **4** and **12** showed the highest growth inhibitory activity against *M. bovis* with a MIC of 0.04 mg/L. On the other hand, thiazole-including PBD-conjugates **3** (Th-Th-PBD) and **11** (Th-Th-Th-PBD) exhibited the lowest growth inhibitory activity against both *M. tuberculosis* and *M. bovis* BCG with values of 5.19 and 20 mg/L, respectively. First-line anti-tubercular drugs isoniazid and rifampin were used as positive controls and inhibited the growth of both mycobacterial strains at 0.05 mg/L.

#### *Antibacterial activity on E. coli K12, P. putida KT2442 and Rhodococcus sp. RHA1*

In order to evaluate the mycobacterial specificity of PBD-conjugates **1-12** in whole cell experiments and determine whether the compounds selectively affected slow-growing mycobacteria in comparison with fast-growing bacteria, we investigated the growth inhibitory activities of **1-12** against Gram-positive *Rhodococcus sp. RHA1* and Gram-negative *Escherichia coli* K12 and *Pseudomonas putida* KT2442 bacteria. The results in **Table 1** show that the majority of PBD-conjugates (**1**, **4-7**, **9**, **10** and **12**) had a significant growth inhibitory activity against *E. coli* and *Rhodococcus sp.* with a MIC value of 1.25 mg/L. Interestingly, PBD-conjugate **8** was 150-fold more active against *M. tuberculosis* (0.32 mg/L) than Gram-negative *E. coli* and *P. putida* (>50 mg/L), whereas thiazole-containing PBD-conjugates **3** and **11** were 10-fold more active against *M. tuberculosis* (5.19 mg/L) than *E. coli*, *P. putida* and *Rhodococcus sp.* (>50 mg/L) strains. Tri-pyrrole-including PBD-conjugate **12** was active against *P. putida* at 5 mg/L, whereas compounds **4** and **5** inhibited the growth of this bacterium at 10 mg/L. Compounds **7**, **9** and **10** were found to be approximately 300-fold more active against *M. tuberculosis* (0.16 mg/L) than *P. putida* (50 mg/L). The aminoglycoside antibiotic kanamycin was used as a positive control and inhibited the growth of *E. coli* and *P. putida* at 1.0 mg/L and *Rhodococcus sp.* at 10 mg/L.

199 *Macrophage RAW264.7 cytotoxicity*

200 The PBD-conjugates displayed various degrees of cytotoxicity against mammalian macrophages  
201 RAW264.7 with GIC<sub>50</sub> values ranging from 1.66 to 4.45 mg/L. The values of the Selectivity Index  
202 (SI), which is the ratio between macrophage half-growth inhibition concentration (GIC<sub>50</sub>) and MIC  
203 against the virulent H<sub>37</sub>Rv strain, ranged from 0.32 to 30.1, with PBD-conjugate **4** (Py-Py-PBD)  
204 exhibiting the highest specificity (SI = 30.1) amongst the library members. PBD-conjugates **5**, **7**, **9**,  
205 **10** and **12** exhibited a SI of 10.4, whereas **1** had a SI of 14.4. Thiazole-including PBD-conjugates **3**  
206 and **11** showed the lowest specificity, with SI values of 0.46 and 0.32, respectively.

207 *DNase I footprinting*

208 DNase I footprinting was used to identify the binding sites of the PBD-conjugates, using the DNA  
209 fragments HexAfor and HexBrev,<sup>28</sup> which together contain all 64 possible symmetrical  
210 hexanucleotide sequences. The results are shown in **Figure 3**. The left hand panels show the  
211 footprints with 10 µM of compounds **2**, **3**, **5**, **7**, **9** and **10** with HexAfor and HexBrev, while the two  
212 panels on the right show examples of the concentration dependence of the footprints with **5** and **9** on  
213 HexAfor. It is evident that compounds **5**, **9** and **10** produced large footprints in both HexAfor and  
214 HexBrev, while compound **7** produced fewer footprints including two shorter footprints (4a and b)  
215 within site 4. Each of these ligands produced a distinct cleavage pattern and the location of the major  
216 footprints is indicated in **Figure 4**. All these compounds contain three rings conjugated to the PBD.  
217 A few weaker footprints were seen with the compounds that only contain two conjugated rings.  
218 Compound **2**, which contains thiazole and pyrrole rings, produced footprints at sites 2, 4 and 8, while  
219 no footprints were seen with **3**, which contains two thiazole rings. It is clear that addition of the  
220 heterocycles affects the interaction of PBD with DNA. PBD-conjugates **5** (Py-Py-Im-PBD), **9** (Py-  
221 Py-Th-PBD) and **10** (Py-Th-Py-PBD) bound to sites 1, 2, 3 and 4 within HexBrev, and to sites 6, 7, 8  
222 and 9 within HexAfor, while the footprint at site 5 in HexBrev is only evident with compounds **5** and  
223 **9**. Compound **7** bound to fewer sites with clear footprints limited to sites 3, 4a and 4b on HexBrev  
224 and site 8 on HexAfor. Although each ligand produced a characteristic cleavage pattern, it is

noticeable that many of the footprints contained a short A/T tract followed by a guanine. The two right hand panels of **Figure 3** show the concentration dependence of the footprints with **5** and **9** on the HexAfor fragment. At 5  $\mu$ M concentration **5** produced a single footprint located in the lower part of site 8 within the sequence 5'-GCGCTTAAGTACT. Compound **9** produced footprints that persisted to lower concentrations, and the protections at the lower part of site 8 and in the centre of site 7 (5'-TAAACGTT) were still evident with 0.5  $\mu$ M ligand.

### *DNA Melting Studies*

In order to further evaluate the contribution of the heterocyclic chains to the DNA recognition properties of the PBD-conjugates, the effects of the ligands on DNA-melting temperature were analysed using two fluorescently-labelled 14-mer DNA duplexes. These AT-rich DNA duplexes contained either a central GGATCC or GTATAC and the results with 0.5  $\mu$ M ligand are shown in **Figure 5**. It can be seen that all four of these ligands stabilised the duplexes and produced transitions at elevated temperatures. Since the ligands were covalently attached to the DNA, the  $T_m$  values of each transition did not change with the ligand concentration. However, the relative proportions of the different components were altered, so that a greater fraction of the higher  $T_m$  was evident with higher ligand concentrations. Each of these duplexes contains more than one guanine with which the conjugates could attach (two guanines for GTATAC and four for GGATCC) and further transitions were observed at higher ligand concentrations, as evident for **10** with both oligonucleotide duplexes. At a concentration of 0.5  $\mu$ M the ligand was in excess of the target duplex (0.25  $\mu$ M). The fraction of the melting transition that has shifted to the higher temperature therefore indicates the proportion of the duplex that has been modified within the incubation period, though the absolute values of the melting transitions indicate the stabilization that is imparted by the bound ligand. The result of these experiments are summarised in **Table 2**. It can be seen that there is a good correlation between the large footprints produced by PBD-conjugates **9** and **10** with their greatest effect on the melting curves. At 0.5  $\mu$ M **9** shifted the entire melting curve to a higher temperature with both GTATAC ( $\Delta T_m = 29$ ) and GGATCC ( $\Delta T_m = 35$ ) with a small amount of uncomplexed duplex (5 and 10%, respectively). A

similar effect is seen with **10** and GTATAC for which about 30% of the transition was shifted to an even higher temperature transition. In contrast, a significant amount of uncomplexed duplex (25%) was still evident with **10** and GGATCC, even though about 20% of the transition corresponded to a higher transition that suggested binding of a second ligand. The melting curves with 0.5  $\mu$ M **5** and **7** contained a large amount of the transition that corresponded to the uncomplexed duplex. **5** and **7** had a similar effect on GGATCC, though a greater fraction of GTATAC was bound by **7**.

#### 4. Discussion

The anti-mycobacterial evaluation of PBD-conjugates **1-12** revealed that these compounds have remarkable growth inhibitory activity against *M. tuberculosis* H<sub>37</sub>Rv. The nature and the length of the polyamide chain attached to the PBD unit had a significant influence on the molecules' anti-microbial activity and DNA-sequence selectivity. The presence of pyrrole rings in the polyamide chains affected the overall anti-tubercular activity of the compounds. The di-pyrrole-containing **4** had a MIC value of 0.08 mg/L, which was comparable to those of isoniazid and rifampin, and an encouraging therapeutic window (SI = 30) that could be further improved in the second generation of PBD-based anti-tuberculosis agents. Although displaying some degrees of cytotoxicity towards mammalian cells, PBD-conjugate **4** represents a promising anti-TB therapeutic lead, particularly in light of the results generated by the large TB drug discovery campaign recently conducted by GlaxoSmithKline (GSK).<sup>29</sup> Researchers at GSK screened a 2 million proprietary-compounds collection for anti-mycobacterial activity against *M. tuberculosis* H37Rv and for cytotoxicity against mammalian cells (HepG2). A set of 177 bioactive-leads were identified displaying MIC <10  $\mu$ M against H37Rv and selectivity (therapeutic) index (SI = HepG2IC<sub>50</sub>/MIC)  $\geq$ 50. These values are of the same order of magnitude of those displayed by **4** (MIC = 0.13  $\mu$ M and SI = 30), thus qualifying this compound as a promising lead that can be improved in subsequent medicinal chemistry work.

In addition, compounds **5, 7, 9, 10** and **12**, which exhibited the second best growth inhibitory activity of the series against the TB causing bacillus (MIC = 0.16 mg/L), all contained at least one pyrrole ring in their three-heterocyclic chains. PBD-conjugates with three-imidazole (**8**) and three-thiazole (**11**)

chains showed a 2-fold and 30-fold decrease in *M. tuberculosis* growth inhibitory activity, respectively. This study also showed that the antimicrobial activity of PBD-conjugates **1-12** was highly selective against slow-growing mycobacteria *M. tuberculosis* and *M. bovis* compared to fast-growing bacteria *E. coli*, *P. putida* and *Rhodococcus sp.* The mechanism of action of the PBDs is unique and involves the covalent binding to guanine residues within the DNA minor-groove. The DNase I footprinting results showed that the PBD-conjugates bound with high affinity to large DNA sequences containing short A/T stretches followed by a guanine residue, with **9** protecting the 5'-TAAACGTT sequence at a concentration as low as 0.5  $\mu$ M. This can be exploited to target discrete DNA sequences within the GC-rich mycobacterial genome and ultimately disrupt key enzymes and transcription factors. DNA melting studies revealed that thiazole-containing **9**, and to a lesser extent **10**, formed strong complexes and markedly shifted the melting curves of the two 14-mer DNA duplexes used in this study, thus confirming the significant DNA stabilisation properties of the compounds. In summary, these results show that **1-12** could serve as DNA-targeted therapeutic leads for the treatment of tuberculosis and further studies are underway to implement the potency and therapeutic index of these compounds.

## Acknowledgements

We thank Professor Siamon Gordon for providing the RAW264.7 cell-line and Professor Simon Croft for granting access to the TB lab in the LSHTM. SB is a Cipla Distinguished Fellow in Pharmaceutical Sciences. Supported by MRC, UK (Grant Code: G0801956 to S.B.) to fund D.E. and T.M.'s post-doctoral studies at Birkbeck, University of London. J.D.G. received financial support from Colfuturo and a Bloomsbury Colleges studentship for his PhD studies. E.M. carried out a PhD rotation in S.B.'s lab funded by a Wellcome Trust Scholarship. M.A.B. is a Commonwealth Scholar in K.R.F.'s lab. The funders had no role in study design, data collection and analysis, decision to publish or preparation of the manuscript.

## References

1. WHO. Global tuberculosis report 2012. Geneva: WHO. (2014)

2. Guzman JD, Gupta A, Bucar F, Gibbons S, Bhakta S. Antimycobacterials from natural sources: ancient times, antibiotic era and novel scaffolds. *Front Biosci.* 17:1861-1881 (2012)
3. Galagan JE, et al. The Mycobacterium tuberculosis regulatory network and hypoxia. *Nature.* 499(7457):178-183 (2013)
4. Denny WA, Abraham DJ. Synthetic DNA-Targeted Chemotherapeutic Agents And Related Tumor-Activated Prodrugs. In Burger's Medicinal Chemistry and Drug Discovery. John Wiley & Sons, Inc., (2003)
5. Cozzi P, Mongelli N, Suarato A. Recent anticancer cytotoxic agents. *Current medicinal chemistry. Anti-cancer agents.* 4(2):93-121 (2004)
6. Hartley JA, Hochhauser D. Small molecule drugs - optimizing DNA damaging agent-based therapeutics. *Current opinion in pharmacology.* 12(4):398-402 (2012)
7. Baraldi PG, et al. DNA minor groove binders as potential antitumor and antimicrobial agents. *Med Res Rev.* 24(4):475-528 (2004)
8. Hartley JA. The development of pyrrolobenzodiazepines as antitumour agents. *Expert opinion on investigational drugs.* 20(6):733-744 (2011)
9. Antonow D, Thurston DE. Synthesis of DNA-interactive pyrrolo[2,1-c][1,4]benzodiazepines (PBDs). *Chemical reviews.* 111(4):2815-2864 (2011)
10. Leimgruber W, Stefanovic V, Schenker F, Karr A, Berger J. Isolation and characterization of anthramycin, a new antitumor antibiotic. *Journal of the American Chemical Society.* 87(24):5791-5793 (1965)
11. Antonow D, et al. Solution structure of a 2:1 C2-(2-naphthyl) pyrrolo[2,1-c][1,4]benzodiazepine DNA adduct: molecular basis for unexpectedly high DNA helix stabilization. *Biochemistry.* 47(45):11818-11829 (2008)
12. Puvvada MS, et al. Inhibition of bacteriophage T7 RNA polymerase in vitro transcription by DNA-binding pyrrolo[2,1-c][1,4]benzodiazepines. *Biochemistry.* 36(9):2478-2484 (1997)
13. Hartley JA, et al. SG2285, a novel C2-aryl-substituted pyrrolobenzodiazepine dimer prodrug that cross-links DNA and exerts highly potent antitumor activity. *Cancer research.* 70(17):6849-6858 (2010)
14. Hartley JA, Hamaguchi A, Suggitt M, Gregson SJ, Thurston DE, Howard PW. DNA interstrand cross-linking and in vivo antitumor activity of the extended pyrrolo[2,1-c][1,4]benzodiazepine dimer SG2057. *Investigational new drugs.* 30(3):950-958 (2012)
15. Rahman KM, et al. Antistaphylococcal activity of DNA-interactive pyrrolobenzodiazepine (PBD) dimers and PBD-biaryl conjugates. *Journal of Antimicrobial Chemotherapy.* 67(7):1683-1696 (2012)
16. Rosado H, Rahman KM, Feuerbaum E-A, Hinds J, Thurston DE, Taylor PW. The minor groove-binding agent ELB-21 forms multiple interstrand and intrastrand covalent cross-links with duplex DNA and displays potent bactericidal activity against methicillin-resistant Staphylococcus aureus. *Journal of Antimicrobial Chemotherapy.* 66(5):985-996 (2011)
17. Rahman KM, et al. GC-Targeted C8-Linked Pyrrolobenzodiazepine-Biaryl Conjugates with Femtomolar in Vitro Cytotoxicity and in Vivo Antitumor Activity in Mouse Models. *J. Med. Chem.* 56(7):2911-2935 (2013)
18. Hadjivassileva T, Thurston DE, Taylor PW. Pyrrolobenzodiazepine dimers: novel sequence-selective, DNA-interactive, cross-linking agents with activity against Gram-positive bacteria. *Journal of Antimicrobial Chemotherapy.* 56(3):513-518 (2005)
19. Pepper CJ, Hambly RM, Fegan CD, Delavault P, Thurston DE. The novel sequence-specific DNA cross-linking agent SJG-136 (NSC 694501) has potent and selective in vitro cytotoxicity in human B-cell chronic lymphocytic leukemia cells with evidence of a p53-independent mechanism of cell kill. *Cancer research.* 64(18):6750-6755 (2004)
20. Antonow D, Jenkins TC, Howard PW, Thurston DE. Synthesis of a novel C2-aryl pyrrolo[2,1-c][1,4]benzodiazepine-5,11-dione library: effect of C2-aryl substitution on cytotoxicity and non-covalent DNA binding. *Bioorganic & medicinal chemistry.* 15(8):3041-3053 (2007)
21. Brucoli F, et al. An extended pyrrolobenzodiazepine-polyamide conjugate with selectivity for a DNA sequence containing the ICB2 transcription factor binding site. *J Med Chem.* 56(16):6339-6351 (2013)

22. Brucoli F, et al. Novel C8-linked pyrrolobenzodiazepine (PBD)-heterocycle conjugates that recognize DNA sequences containing an inverted CCAAT box. *Bioorganic & medicinal chemistry letters*. 21(12):3780-3783 (2011)
23. Wells G, et al. Design, synthesis, and biophysical and biological evaluation of a series of pyrrolobenzodiazepine-poly(N-methylpyrrole) conjugates. *J Med Chem*. 49(18):5442-5461 (2006)
24. Dervan PB. Molecular recognition of DNA by small molecules. *Bioorganic & medicinal chemistry*. 9(9):2215-2235 (2001)
25. Brucoli F, Guzman JD, Maitra A, James CH, Fox KR, Bhakta S. Synthesis, anti-mycobacterial activity and DNA sequence-selectivity of a library of biaryl-motifs containing polyamides. *Bioorganic & Medicinal Chemistry*. 23(13):3705-3711 (2015)
26. Guzman JD, et al. Antitubercular specific activity of ibuprofen and the other 2-arylpropanoic acids using the HT-SPOTi whole-cell phenotypic assay. *BMJ Open*. 3(6) (2013)
27. Danquah CA, Maitra A, Gibbons S, Faull J, Bhakta S. HT-SPOTi: A Rapid Drug Susceptibility Test (DST) to Evaluate Antibiotic Resistance Profiles and Novel Chemicals for Anti-Infective Drug Discovery. *Current protocols in microbiology*. 40:17 18 11-17 18 12 (2016)
28. Hampshire AJ, Fox KR. Preferred binding sites for the bifunctional intercalator TANDEM determined using DNA fragments that contain every symmetrical hexanucleotide sequence. *Analytical biochemistry*. 374(2):298-303 (2008)
29. Ballell L, et al. Fueling Open-Source Drug Discovery: 177 Small-Molecule Leads against Tuberculosis. *Chemmedchem*. 8(2):313-321 (2013)

## Figure Legends

**Figure 1.** Schematic representation of the mechanism of action of PBDs involving the nucleophilic attack of the C2-NH<sub>2</sub> group of a guanine residue to the N10-C11 imine moiety of PBD within the DNA minor groove.

**Figure 2.** The library of twelve C8-linked PBD-heterocyclic polyamide conjugates **1-12** tested in this study.

**Figure 3.** DNase I footprinting patterns of the PBD-conjugates on the HexBrev and HexAfor DNA fragments. The first two panels show the results in the presence of 10 µM of each of the PBD-conjugates. The second two panels show the concentration dependence of footprints on HexAfor with **5** and **9**. Ligand concentrations (µM) are shown above each gel lane. The bars indicate the location of clear footprints. Tracks labelled GA are sequence markers specific for G and A, while con indicates DNase I cleavage in the absence of added ligand.

**Figure 4.** Sequences of HexAfor and HexBrev indicating the location of binding sites of the PBD-conjugates (underlined and numbered in sequences).

**Figure 5.** Fluorescence melting profiles for the DNA duplexes 5'-F-AAAAGGATCCAAAA/5'-TTTTGGATCCTTTT-Q and 5'-F-AAAAGTATACAAAA/5'-TTTTGTATACTTTT-Q (F = fluorescein and Q = dabcy). The ligand concentration was 0.5 µM with 0.25 µM target duplex.



## Figures

Figure 1

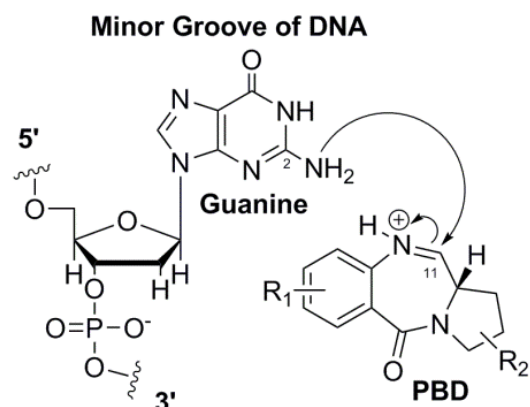
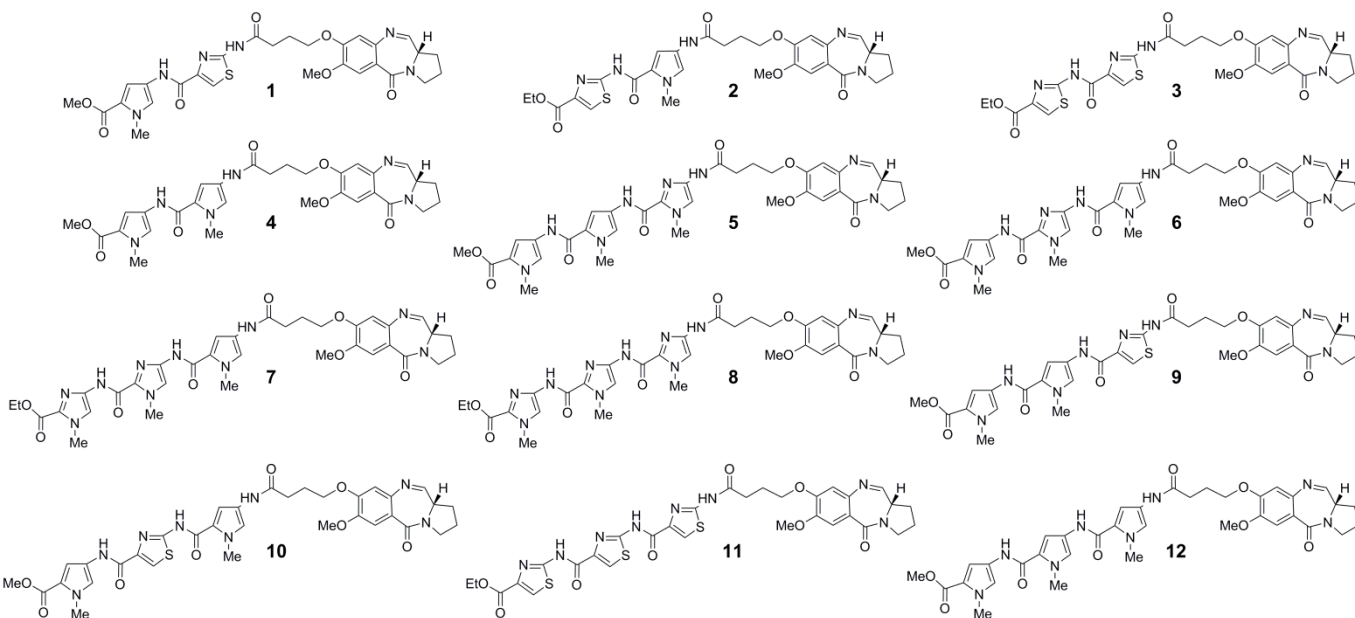
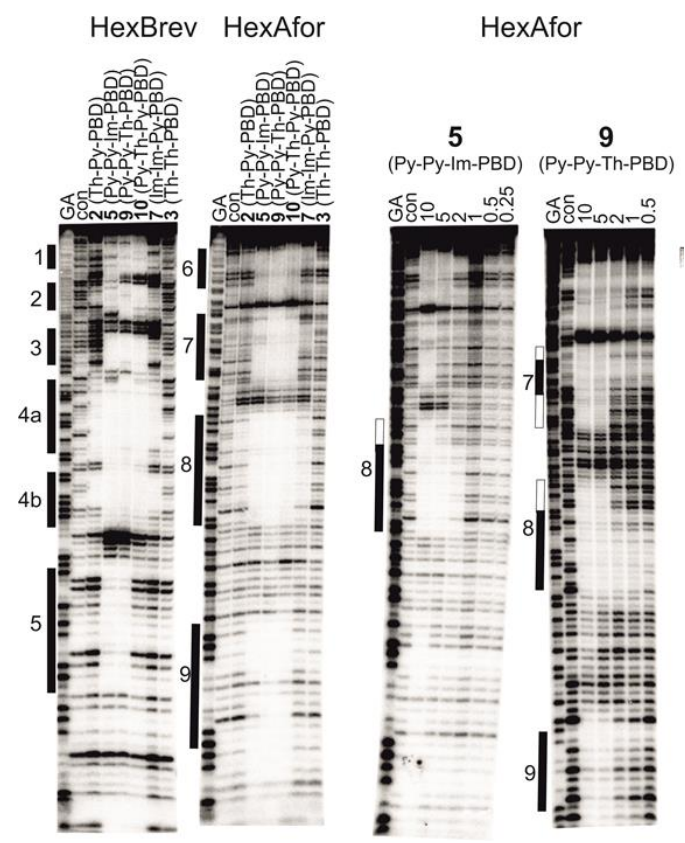


Figure 2



432 **Figure 3**



433

434

435

436

437

438

439

**Figure 4**

**HexBrev**  
5'-...GGATCCATGCATT AATTCGAATATTGATCATGACGTGACACA TGTACATATGTATATACG  
1 2  
CGCGTACGC GTATACGTAGCGCGCTT ATAAGCTTGCAATTGCCGGCT AATTAGGGCCCTC  
3 4a 4b  
GAGCTCGCGATCGGCCGGATCC-3'  
5

**HexAfor**  
5'-...GGATCCCGGGATATCGATATA TGGCGCCAAATTTAGCTATAGATCTAGAATTCCGGACC  
6  
GCGGTTTAAACGTTAACCGGTACCTAGGCCTGCAGCTGC GCATGCTAGCGCTTAAGTACTAG  
7 8  
TGCACGTGGCCA TGGATCC-3'  
9

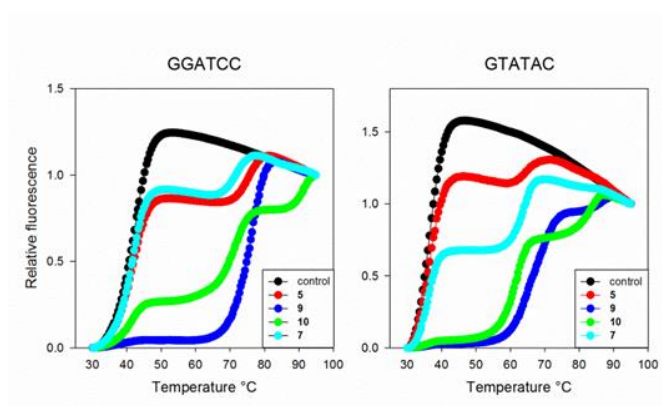
440

441

442

443

**Figure 5**



## Tables

**Table 1.** Biological activity of PBD-conjugates **1-12**.

Compound	MICs (mg/L)					GIC <sub>50</sub> RAW264.7 (mg/L)	SI <sup>a</sup>
	<i>Mycobacterium tuberculosis</i> H <sub>37</sub> Rv	<i>Mycobacterium bovis</i> BCG	<i>Escherichia coli</i> K12	<i>Pseudomonas putida</i> KT2442	<i>Rhodococcus</i> sp. RHA1		
<b>Py-Th-PBD (1)</b>	0.31	0.16	1.25	>20	1.25	4.45	14.4
<b>Th-Py-PBD (2)</b>	0.63	0.63	2.5	>50	5.0	2.41	3.83
<b>Th-Th-PBD (3)</b>	5.19	<20	>50	>50	>50	2.41	0.46
<b>Py-Py-PBD (4)</b>	0.08	0.04	1.25	10.0	1.25	2.41	30.1
<b>Py-Py-Im-PBD (5)</b>	0.16	0.16	1.25	10.0	1.25	1.66	10.4
<b>Py-Im-Py-PBD (6)</b>	0.32	<20	1.25	50.0	1.25	1.66	5.19
<b>Im-Im-Py-PBD (7)</b>	0.16	0.08	1.25	>50	1.25	1.66	10.4
<b>Im-Im-Im-PBD (8)</b>	0.32	<20	50.0	>50	10.0	1.66	5.19
<b>Py-Py-Th-PBD (9)</b>	0.16	0.08	1.25	50.0	1.25	1.66	10.4
<b>Py-Th-Py-PBD (10)</b>	0.16	0.08	1.25	>50	1.25	1.66	10.4
<b>Th-Th-Th-PBD (11)</b>	5.19	ND	>50	>50	>50	1.66	0.32
<b>Py-Py-Py-PBD (12)</b>	0.16	0.04	1.25	5.0	1.25	1.66	10.4
<b>Isoniazid</b>	0.05	0.05	ND	ND	ND	3000	60000
<b>Rifampin</b>	0.05	0.05	ND	ND	ND	700	14000
<b>Kanamycin</b>	ND	ND	1.0	1.0	10.0	ND	ND

<sup>a</sup>The SI was calculated by dividing the GIC<sub>50</sub> for RAW264.7 by the MIC against *M. tuberculosis* H<sub>37</sub>Rv

**Table 2.** Changes in melting temperature ( $\Delta T_m$ ) of the oligonucleotide duplexes in the presence of 0.5  $\mu$ M of each ligand and the fraction of the transition that corresponds to the uncomplexed duplex.

	GGATCC $T_m = 41.7^\circ\text{C}$		GTATAC $T_m = 36.4^\circ\text{C}$	
	$\Delta T_m$	% free	$\Delta T_m$	% free
Py-Py-Im-PBD ( <b>5</b> )	33	75	28	80
Im-Im-Py-PBD ( <b>7</b> )	30	80	28	55
Py-Py-Th-PBD ( <b>9</b> )	35	10	29	5
Py-Th-Py-PBD ( <b>10</b> )	31	25	26	0

